Feedback-Receiver-Based Compensation of Nonlinearities in Trapped Ion Qubit Gate Signaling

Moritz Baecker, Marvin Jaeger, Bartosz Tegowski, Georg F. Riemschneider, Alexander Koelpin
Institute of High-Frequency Technology, Hamburg University of Technology, Germany
marvin.jaeger@tuhh.de

2026 17th German Microwave Conference (GeMiC) | 979-8-3195-1955-9/26/$31.00 ©2026 IEEE | DOI: 10.1109/GeMiC71240.2026.11516472

***Abstract*— This paper presents an analog microwave frontend designed to downconvert and feed back the control signal for trapped ion qubits, which are frequency-multiplexed by the magnetic gradient induced coupling (MAGIC) principle. Shorter gate durations require a higher excitation signal power, increasing distortion caused by nonlinear components. The proposed feedback receiver serves the purpose of coupling out a portion of the generated qubit control signal to feed it back into the signal generation hardware. This enables closed-loop signal processing techniques to compensate for nonlinearities in signal generation, thus improving the idle fidelity of untargeted qubits. The characterization of a manufactured prototype is performed, followed by an active cancellation of spurious tones based on the downconverted qubit control signal to demonstrate the capability for qubit fidelity improvement.**

***Keywords*— Fidelity, magnetic gradient induced coupling (MAGIC), microwave frontend, receivers, quantum computing, qubit.**

I. Introduction

In recent years, quantum computing has gained popularity as a promising approach to speed up certain kinds of computing problems [1], [2]. Various concepts for the physical implementation are subject to current research, e.g., trapped ions [3], photonic quantum systems [4], semiconductor spin qubits [5], as well as superconducting circuits [6]. In quantum computers, qubits are the information storage unit in analogy to bits known from classical computers. The advantage is that a qubit can exist in a continuum of superposition states between the basis states $|0\rangle$ and $|1\rangle$ as long as not being evaluated by measurement. Thus, a sequence of manipulations can lead to intended superposition states, which are then evaluated to gain information about the probability distribution of the measurable basis states [7].

Trapped ion qubits can be controlled by being exposed to oscillating magnetic fields originating from radio frequency (RF) signals at specific frequencies. The magnetic field gradient induced coupling (MAGIC) concept aims to scale up this approach by shifting multiple qubit excitation frequencies using a static magnetic field gradient [9], [10]. This concept is illustrated in Fig. 1(a) and allows to control individual qubit states simultaneously with a frequency multiplexed signal.

The signal generation for this purpose poses challenges from a microwave engineering perspective. Frequency spurs caused by nonlinear components can coincide with excitation frequencies of neighboring qubits, thus degrading their fidelity [11]. To compensate for this, linearization techniques are

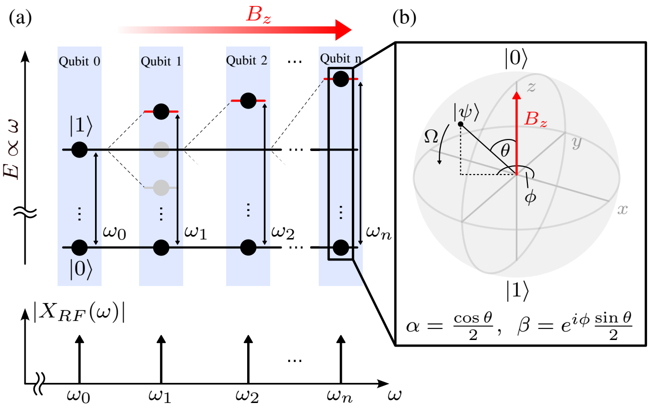

Fig. 1. (a) Illustration of multiple MAGIC-based trapped-ion qubits. The Zeeman effect splits up the excited energy states $|1\rangle$ depending on the local static magnetic field B_z. (b) Qubit state $|\psi\rangle$ on the Bloch sphere with indicated Rabi oscillation at frequency Ω. Adapted from [8].

applicable, requiring the integration of a feedback loop into the signal generation hardware [12, p. 316].

This paper proposes a feedback receiver to provide feedback signals by coupling out and downconverting a fraction of the RF qubit control signal. A manufactured feedback receiver prototype is designed and characterized. Its functionality is demonstrated by an active cancellation of spurious spectral components.

Section II introduces qubit manipulation mechanisms relevant from the microwave engineering perspective. Section III explains the feedback receiver design. Its characterization follows in Section IV and Section V deals with a proof-of-concept demonstration. Section VI summarizes this paper.

II. Qubit Theory

To understand the requirements for a qubit control signal receiver, the interaction between electromagnetic signals and qubits is summarized. For further details, see [7]. Trapped ions offer the capability to implement qubits due to their discrete energy states, which can represent qubit basis states denoted as $|0\rangle$ for the ground state and $|1\rangle$ for the excited state. The general form of a qubit state is defined as $|\psi\rangle = \alpha \cdot |0\rangle + \beta \cdot |1\rangle$, where α and β are complex probability amplitudes, normalized with $|\alpha|^2 + |\beta|^2 = 1$. Qubit states are commonly visualized on the Bloch sphere, depicted in Fig. 1(b).

A. Qubit State Manipulation

To achieve controlled manipulations of a quantum state, the qubit is exposed to a magnetic field oscillating at an excitation frequency proportional to the energy difference between its two considered basis states. The selected ion species $^{171}Yb^{+}$ used for MAGIC has a state separation that corresponds to excitation frequencies around $12.64\,\mathrm{GHz}$ [9]. This results in an oscillation of the qubit state between the two basis states at the so-called Rabi frequency Ω, which is in turn proportional to the amplitude of the applied oscillating magnetic field [7]. In Fig. 1(b), Ω is indicated as rotation rate of state $|\psi\rangle$ along θ. By exciting Rabi oscillations for specific durations, arbitrary qubit states can be reached [7].

Among other techniques, multiple qubits can be simultaneously controlled by the MAGIC principle [9], which is visualized in Fig. 1(a). It relies on the Zeeman effect, causing a static magnetic field at the location of an ion—in this case in z-direction—to split its excited basis state into three basis states, with the highest or lowest taken as the new excited basis state $|1\rangle$. Since this effect depends on the field strength, a gradient of the static magnetic field along a chain of ions leads to a unique shift in excitation frequency for each individual qubit, making multiple qubits controllable with a frequency-multiplexed signal $X_{RF}(\omega)$, as shown generically in Fig. 1(a).

B. Control Signal Implications

Nonlinear behavior in the signal generation hardware distorts the ideal signal $X_{RF}(\omega)$, for instance, by introducing spurious harmonic tones or intermodulation products. These spurious tones degrade the idle fidelity F of untargeted qubits, once they coincide with the respective excitation frequencies. In quantum mechanics, fidelity is a measure for the similarity of two states, the real and the desired one. An alternative expression is the infidelity $1 - F$. Idle fidelity describes how accurately a qubit state is maintained while not being purposely manipulated. According to [8], the worst-case idle fidelity of an untargeted qubit excited by a π-pulse

$$F = 1 - \frac{\pi^2}{4 \cdot \mathrm{SFDR}} \tag{1}$$

is determined by the spurious-free dynamic range (SFDR). It is assumed that the largest spur is located at the excitation frequency of the evaluated qubit.

III. Feedback Receiver Design

The MAGIC-compliant qubit control signal follows an in-phase-quadrature (IQ) signaling scheme to allow independent single-sideband (SSB) modulation of both upper- (USB) and lower sideband (LSB). A microwave frontend capable of generating such signals is presented in [8] and has a maximum bandwidth of $600\,\mathrm{MHz}$. Since linearization techniques, e.g., digital predistortion (DPD) [13], require information about intermodulation products, higher feedback bandwidths are desirable, leading to a chosen design bandwidth of $2\,\mathrm{GHz}$ centered at $12.64\,\mathrm{GHz}$ for the feedback receiver.

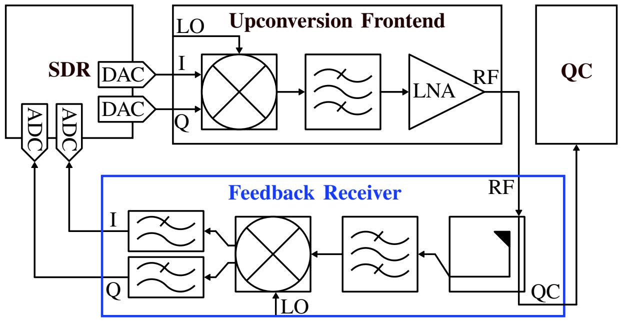

Fig. 2. Block diagram of a qubit control signal generation system including the proposed feedback receiver and a connected quantum computer (QC).

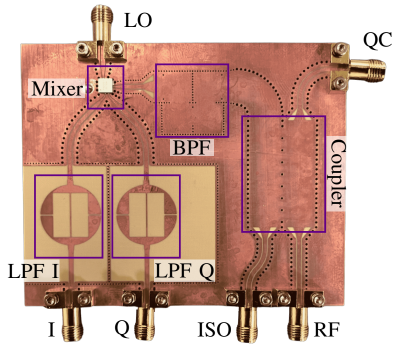

Fig. 3. Manufactured feedback receiver on a printed circuit board.

Fig. 2 depicts a block diagram of the proposed architecture, implementing a feedback downconversion stage for the qubit control signal. It consists of a coupler, a bandpass filter (BPF), an IQ mixer, and, at each intermediate frequency (IF) output, a lowpass filter (LPF). The two IF outputs of the mixer are fed back into analog-to-digital converters (ADCs) of a software-defined radio (SDR).

The manufactured analog frontend implementing the feedback receiver is shown in Fig. 3. The RF signal enters the multihole substrate integrated waveguide (SIW) coupler at the RF port. Around $-10\,\mathrm{dB}$ are coupled into the subsequent SIW corner cavity BPF design from [14], which filters the mixer input with $2\,\mathrm{GHz}$ bandwidth while providing an improved stopband at twice the frequency band of interest to suppress fourth-order intermodulation products. The main signal available at the QC port can be used to control qubits after experiencing an insertion loss from the coupler of $2\,\mathrm{dB}$. A matched load terminates the isolated port (ISO). The output of the BPF is fed into an IQ mixer (*Qorvo QPX0001*), for which a high linearity is desirable to avoid additional intermodulation products. According to the datasheet, the mixer introduces a conversion loss of approximately $8\,\mathrm{dB}$, has an input third-order intercept point (IIP3) of around $21\,\mathrm{dBm}$ and an isolation from local oscillator (LO) to RF better than $40\,\mathrm{dB}$. The IQ outputs of the mixer are followed by a circular patch LPF from [15] each, having an elliptic function characteristic and an improved stopband performance to suppress aliasing effects.

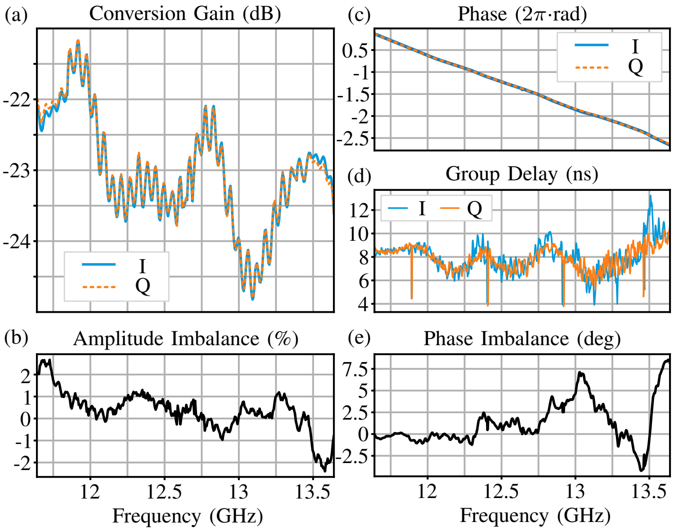

Fig. 4. Characterization results. (a) Conversion gain and (b) relative magnitude error of Q with respect to I. (c) Phase response, (d) group delay, and (e) phase imbalance of Q with respect to I.

IV. Characterization

In the following, the performance of the proposed microwave frontend is evaluated in terms of conversion gain, phase response, and IQ imbalances. For the conversion gain of the receiver, a scalar three-port frequency conversion measurement with a vector network analyzer (VNA) (*Rohde & Schwarz ZVA50*) is performed. The RF signal is swept from 11.64 GHz to 13.64 GHz at a power of 10 dBm. A 17 dBm LO signal drives the mixer at 12.64 GHz. The conversion gain is plotted in Fig. 4(a) and takes on values between −21 dB and −25 dB in the desired passband. A maximum gain imbalance between I and Q of 2.7 % is observed, as shown in Fig. 4(b).

To measure the phase response of the mixer, an RF one-port measurement is performed as described in [16], which is based on terminating one IF port under test with known load standards from an open, short, load (OSL) calibration kit. The second IF port is terminated by a matched load. This procedure is subject to the assumption that the receiver acts as a linear, reciprocal system, which is justified by prior measurements of the overall receiver system. In these measurements, sufficiently low nonlinear distortion with an SFDR better than 40 dBc at the maximum specified input power of 10 dBm and an IIP3 of 48 dBm were observed.

Fig. 4(c)–(e) shows the phase measurement results, evaluated as phase response in Fig. 4(c), group delay in Fig. 4(d) and as phase imbalance in Fig. 4(e). For higher frequencies, the phase imbalance takes on values up to 8°. The RF frequency of 12.64 GHz—corresponding to a downconversion to dc—is excluded from the measurement, as the IF side does not provide a meaningful phase.

V. Proof-of-Concept Demonstration

As an exemplary demonstration of the functionality of the feedback receiver, nonlinear behavior introduced during qubit control signal generation is actively compensated solely based on the information gained from the receiver's downconverted output signals. To evaluate the improvement of the qubit control signal, particular focus is placed on the second harmonic of the intended excitation frequency. It is assumed that this harmonic tone coincides with the excitation frequency of a neighboring qubit, thereby reducing its idle fidelity. Fig. 5 shows a block diagram of the setup used in this experiment. The analog frontend proposed in [8] is used to upconvert the IF signal generated by signal source S1 from 9 MHz to 12.655 GHz following a USB-SSB modulation scheme. This single-tone signal is dedicated to excite a qubit at an excitation frequency of 12.655 GHz. However, the nonlinearity of the upconversion frontend distorts the near-ideal single-tone signal, introducing its second harmonic at 18 MHz offset from the LO frequency. Signal source S2 uses the same SSB scheme as S1, but at 18 MHz to cancel the harmonic tone. Both IF signals from S1 and S2 are generated in quadrature and are added with power combiners (*Mini-Circuits ZFSC-2-4*). S3 introduces dc bias to the generated IF signals via bias tees (*Mini-Circuits ZFBT-4R2GW-FT+*) to actively suppress the local oscillator leakage (LOL). Signal sources S1, S2, and S3 are all of type *Keysight 33500B*. The LO deviates from the previously mentioned 12.64 GHz by 6 MHz to prevent the signal image from coinciding with a lower allowed energy state of the qubit. The RF signal generated by the upconversion frontend is fed into the RF port of the feedback receiver, with the majority of signal power being transmitted to the QC port. Fig. 6(b) displays the spectrum measured with the spectrum analyzer *Rohde & Schwarz FSUP* connected to that port. The decoupled portion of the signal is downconverted with an LO at 12.616 GHz. The IQ outputs of the receiver are observed using an SDR (*AMD XCZU48DR*), providing the downconverted IF spectrum plotted in Fig. 6(a). The downconversion LO deviation was introduced to move the IF band of interest above 10 MHz which is the lower frequency limit specified for the SDR.

Now, while only observing the downconverted IF spectrum, signal sources S1, S2, and S3 could be tuned to compensate for spurious tones in the upconverted RF spectrum. The first step is to tune the amplitudes and phases of both channels

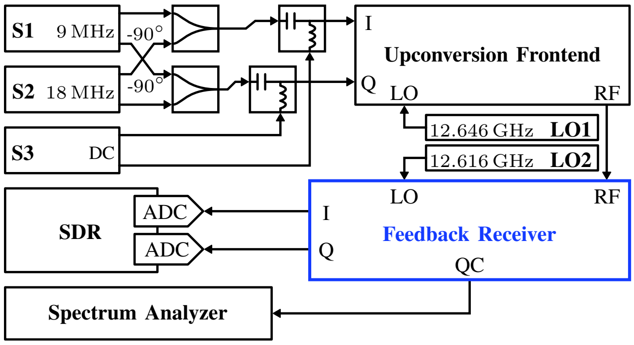

Fig. 5. Measurement setup for the proof-of-concept measurement demonstrating the active compensation of nonlinearities of the upconversion frontend based on the feedback receiver output signal.

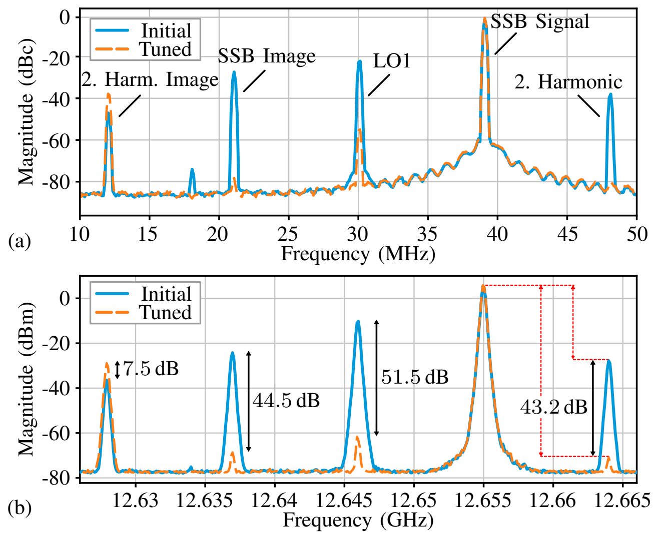

Fig. 6. USB-SSB modulated signal spectrum (a) measured with the SDR at IF and (b) measured with the spectrum analyzer at RF.

on S1 to achieve optimal sideband rejection at 21 MHz, as seen in Fig. 6(a). After that, dc voltages provided by S3 are tuned to minimize the LOL. Finally, a cancellation of the second harmonic located at 48 MHz can be achieved by adding an 18 MHz tone generated by S2. The final tuned spectrum captured at IF is plotted in Fig. 6(a).

Up to this point, only the IF spectrum measured by the SDR was observed. The final evaluation, on the other hand, is based on the RF spectrum measured at the QC port and shown in Fig. 6(b). By calculating the idle infidelity at 12.664 GHz for an initial SFDR of 33.4 dBc as 0.0011, compared to $5{\cdot}10^{-8}$ at a final SFDR of 76.5 dBc, the worst-case idle infidelity due to spurs could be reduced by 99.996 %. This demonstrates the potential effectiveness of feedback-based active cancellation in the context of qubit signaling. Additionally, the LOL has been reduced by 51.5 dB and the control signal image suppression was improved by 44.5 dB.

During the manual tuning, no parameter configuration could be found that further increased the image suppression of the cancellation tone generated by S2, while maintaining the previous improvements. This results in an SFDR degradation by 7.5 dB at 12.628 GHz, as highlighted in Fig. 6(b). In principle, this deviation from the initial power level could be mitigated based on the SSB modulation capability of the cancellation tone. However, the nonlinearity of the upconversion frontend complicates interactions between multiple tones, especially if these tones are multiples of one another. This highlights the necessity for advanced signal control techniques such as DPD.

VI. Conclusion

This work proposes a receiver design enabling a closed feedback loop for qubit control signal generation systems. An exemplary implementation of the receiver has been manufactured and the results of characterization measurements as well as a proof-of-concept demonstration of feedback-based active cancellation are presented. By tuning the qubit control signal based on the downconverted spectrum, the second harmonic of the intended excitation tone could be reduced by 43.2 dB, translating to an estimated idle infidelity reduction by 99.996 %. Furthermore, the image suppression of the intended excitation tone was improved by 44.5 dB and an injection of dc biases before the upconversion mixer reduced the LOL at RF by 51.5 dB. The proposed feedback receiver implements a prerequisite for advanced feedback linearization techniques enabling significant fidelity improvements for qubit signaling.

Acknowledgment

This project was made possible by DLR Quantum Computing Initiative enabled with funding from the Federal Ministry of Research, Technology and Space. https://qci.dlr.de/qsea-ii

References

[1] P. W. Shor, “Polynomial-time algorithms for prime factorization and discrete logarithms on a quantum computer,” *SIAM J. Comput.*, vol. 26, no. 5, pp. 1484–1509, Oct. 1997.

[2] L. K. Grover, “A fast quantum mechanical algorithm for database search,” in *Proc. of the 28th Annu. ACM Symp. on Theory of Comput. (STOC)*, Philadelphia, PA, USA, May 1996, pp. 212–219.

[3] C. D. Bruzewicz, J. Chiaverini, R. McConnell, and J. M. Sage, “Trapped-ion quantum computing: Progress and challenges,” *Appl. Phys. Reviews*, vol. 6, no. 2, p. 021 314, Jun. 2019.

[4] J. L. O’Brien, A. Furusawa, and J. Vučković, “Photonic quantum technologies,” *Nature Photon.*, vol. 3, no. 12, pp. 687–695, Dec. 2009.

[5] A. S. Dzurak, “Spin-based quantum computing in silicon CMOS-compatible platforms,” in *IEEE Int. Electron Devices Meeting (IEDM)*, San Francisco, CA, USA, Dec. 2016, pp. 13.2.1–13.2.2.

[6] P. Krantz, M. Kjaergaard, F. Yan, T. P. Orlando, S. Gustavsson, and W. D. Oliver, “A quantum engineer’s guide to superconducting qubits,” *Appl. Phys. Reviews*, vol. 6, no. 2, p. 021 318, Jun. 2019.

[7] J. C. Bardin, D. Sank, O. Naaman, and E. Jeffrey, “Quantum computing: An introduction for microwave engineers,” *IEEE Microw. Mag.*, vol. 21, no. 8, pp. 24–44, Aug. 2020.

[8] M. Jaeger, G. F. Riemschneider, N. Weiß, B. Tegowski, and A. Koelpin, “Design of a microwave frontend for a trapped ion quantum computer,” in *Proc. 16th Ger. Microw. Conf. (GeMiC)*, Dresden, Germany, Mar. 2025, pp. 152–155.

[9] A. Khromova et al., “Designer spin pseudomolecule implemented with trapped ions in a magnetic gradient,” *Phys. Rev. Lett.*, vol. 108, no. 22, p. 220 502, Jun. 2012.

[10] M. Johanning, A. Braun, N. Timoney, V. Elman, W. Neuhauser, and C. Wunderlich, “Individual addressing of trapped ions and coupling of motional and spin states using RF radiation,” *Phys. Rev. Lett.*, vol. 102, no. 7, p. 073 004, Feb. 2009.

[11] J. Van Dijk et al., “Impact of classical control electronics on qubit fidelity,” *Phys. Rev. Applied*, vol. 12, no. 4, p. 044 054, Oct. 2019.

[12] B. Razavi, in *RF Microelectronics*, 21. printing, 2. Upper Saddle River, NJ: Prentice Hall PTR, 2009.

[13] M. Jaeger, B. Tegowski, G. F. Riemschneider, and A. Koelpin, “Digital predistortion of power amplifiers for quantum computing,” 2026. arXiv: 2601.06524.

[14] T. Jaschke, B. Rohrdantz, J.-P. Mohncke, and A. F. Jacob, “A Ka-band substrate-integrated waveguide diplexer with wide frequency spread,” in *Proc. 46th Eur. Microw. Conf. (EuMC)*, London, United Kingdom, Oct. 2016, pp. 779–782.

[15] Jianpeng Wang, Bing-Zhong Wang, Ye-Hai Bi, and Wei Shao, “Compact circular patch lowpass filter,” in *Proc. IEEE Antennas Propag. Soc. Int. Symp.*, vol. 1B, Washington, DC, USA, Jul. 2005, pp. 606–609.

[16] J. Dunsmore, “Novel method for vector mixer characterization and mixer test system vector error correction,” in *IEEE MTT-S Int. Microw. Symp. Dig.*, vol. 3, Jun. 2002, pp. 1833–1836.